International Journal of Nanomaterials and Chemistry

http://dx.doi.org/10.18576/ijnc/040101

Sonochemical Synthesis, Spectroscopic Characterization, 3D Molecular Modeling, DNA Binding and Antimicrobial Evaluation of some Transition Metal Complexes Based on Bi-dentate NO Donor Imine Ligand

Laila H. Abdel Rahman, Ahmed M. Abu-Dief, Rafat M. El-Khatib and Shimaa Mahdy Abdel-Fatah*

Chemistry Department, Faculty of Science, Sohag University, 82534Sohag, Egypt

Received: 21Sep 2017, Revised: 28 Nov. 2017, Accepted: 1 Dec. 2017.
Published online: 1 Jan. 2018.

Abstract: Some novel Schiff base metal complexes of Cu(II), Co(II), Ni(II) and Fe(II) derived from 2-amino-3-hydroxypyridine and 4-nitrobenzaldehyde were synthesized sonochemically. These complexes were identified by elemental analysis, molar conductance, magnetic Characteristics, thermal analysis, IR, computationally by Molecular 3D modeling and UV-Vis spectra. The stoichiometry and stability constants of the prepared complexes have been evaluated spectrophotometrically. Collected data revealed that all the complexes offered 1:2 (metal: ligand) ratio and the ligand coordinates with the metal ions in a bi-dentate manner in octahedral geometry according to the general formula [M (ahpnb)2.2H2O].nH2O. Thermal data showed the degradation pattern of the complexes. The thermal manner of the metal complexes showed that the hydrated complexes lose water molecules of crystallization in the first step then water molecules of coordination; with decomposition of the ligand molecules in the subsequent stages. Moreover, the investigated compounds were tested against different types of bacteria and fungi. Furthermore, DNA binding of these complexes was tested by using electronic spectra, hydrodynamic measurements and gel electrophoresis. The experimental results explained that the tested complexes could attach to DNA via intercalative mode and showed a various DNA binding potency according to the sequence: ahpnbFe> ahpnbCu> ahpnbNi> ahpnbCo.
Keywords: Sonochemical synthesis, thermal analyses, gel electrophoresis, Antimicrobial activity, DNA interaction.

1 Introduction

Schiff base compounds (–RC=N–) are usually created by the condensation of a primary amine with an active carbonyl. The cross-linking factors can also be obtained from metal complexes with O, N or S ligands. Salicylates or anthranilates and aliphatic or aromatic amines can form cogent five- or six-membered chelate rings which are capable of production metal containing cross-linking factors with the required properties [1-4]. Mortality raise caused by infectious diseases is directly related to the bacteria that possess multiple resistances to antibiotics. The development of new antibacterial drugs which are opulent by innovatory and more active mechanisms of action is clearly an urgent medical need [5]. Schiff bases are identified as promising antibacterial agent similarly, a heterocyclic nucleus, namely pyridine based ligands, have also been used in many biochemical reactions to set and develop molecular systems of biological and medical importance. Earlier work reported that some drugs showed higher activity when administered as metal complexes rather than as organic compounds [6-10]. Metal complexes have received great attention recently, due to their interesting Characteristics in the field of material science and biological systems. Electrical and magnetic Characteristics of metals and metalloids can be tailored by their reaction with various ligands. A huge number of Schiff bases and their complexes may show characteristics such as reversible binding of oxygen, transfer of an amino group, thermal, varied complexing/ redox abilities, and as nano precursors. The Schiff bases have great affinity for transition metal ions; hence show potential applications in various fields. Metal complexes are also suitable as molecular materials, because of the electronic Characteristics connected with the metal centers [11]. The binding of transition metal complexes with DNA is of importance for both therapeutic and scientific reasons [12,13]. Schiff bases are potential anticancer drugs and

* Corresponding author E-mail: ahmed_benzoic@yahoo.com

when connected with their metal, the anticancer dynamism of these complexes is enhanced in comparison to that of the liberated ligand. Schiff base metal complexes of Cr(III), Co(II), Ni(II) and Cu(II) created from 2-[(5-bromo-2-hydroxybenzylidene)amino]pyridin-3-ol [BSAP] and [5-chloro-2-[((2-hydroxy-1-naphthyl)methylene)amino]phenyl]-phenylmethanone (HNAC) were synthesized by conventional route[14]. Schiff base complexes of Cr (III), Co(II), Ni(II) and Cu(II) created from(5-bromosalicylaldhyde) with(2-amino-5-nitrothiazole)[L1H] and 4-dimethylaminobenzaldehyde with 2-amino-3-hydroxypyridine [L2H] have been synthesized by conventional method too . Pyridine derivatives play important role in many biochemical reactions. The molecular patterns having chelating molecular designing and combination pyridine ring have been checked in the field of mycology for the development of metal based drugs. Some efforts have been carried out to set and development of these drugs with pyridine based molecular devices [15-19].The present aim of the work is to use Sonochemical method to synthesize some new Schiff base complexes derived from 2-amino-3-hydroxypyridine and 4-nitrobenzaldehyde, characterized them and examined their antibacterial and anti-fungal potencies. Furthermore, we examined their interaction with DNA to predict the possibility of using them as anti-cancer agents.

2 Experimental

All the starting materials of chemicals used in this investigation Such as 4-nitrobenzlaldehyde (nb), 2-amino-3-hydroxypyridine, the metal salt (Cu(CH3COO)2.H2O,Co(NO3)2.6H2O, Ni(NO3)2,FeSO4.(NH4)2SO4.6H2O), Calf thymus DNA[CT DNA] and Tris[hydroxymethyl]-aminomethane(Tris)were obtained from Sigma–Aldrich Chemie (Germany).Spectroscopic degree ethanol and HCl products were used.

2.1 Conventional Synthesis of Schiff Base Ligand

The Schiff bases have been synthesized by the condensation of equimolar ratio of 4-nitrobenzlaldehyde (1.51 g, 10 mmol) with 2-amino-3-hydroxypyridine (1.10 g, 10 mmol) dissolved in ethanol. The reaction blend was stirred well, refluxed for 3-4 hours and then allowed to cool till room temperature. The colored solid precipitate of Schiff base obtained was filtered, irrigated with cold ethanol many times and drained off under reduced pressure in a desiccator. The purity of tested compounds was examined by TLC using silica gel G (yield: 81 %) as shown in (scheme.1).

2.2 Sonochemical Synthesis of Metal Complexes

Ten milli liters of a 0.1 M ethanol solution of the different metal salts [Co(NO3)2.6H2O/ Ni(NO3)2.6H2O/ Cu(CH3COO)2.H2O/ FeSO4.(NH4)2SO4.6H2O]was positioned in a large-density ultrasonic probe, operating at 24 kHz with a maximum force output of 400 W. Into this solution, 10 ml of 0.2 M solution of the ahpnb ligand (0.486 g) was added drop wise. The obtained precipitate was filtered off, rinsed with ethanol and then dried in air (yield: 65-76%) as shown in (Scheme.2).

2.3 Physical Measurements

Melting point for Schiff base ligand and decomposition points for complexes were carried out on a melting point tool, Gallenkamp, England.IR spectra of the metal complexes in KBr pellets in the range of 4000-400 cm-1 were recorded making use of Shimadzu FTIR model 8101spectrophotometer. Molar conductivity measurements were carried out utilizing JENWAY conductivity meter model 4320 at 298 Kutilizing ethanol as solvent. UV-visible spectra in DMF were registered using 10 mm matched quartz cells on PG spectrophotometer model T+80.1HNMR spectra was registered in DMF on BRUKER model 400 MHz using TMS as an internal standard (δ ppm) and DMSO-d6 as the solvent. The presented Schiff base ligand and their complexes were subjected to (C, H and N) elemental test which was implemented at the analytic unit of the main laboratory of Cairo University by Elemental analyzer Perkin-Elmer model240c.The magnetic measurements were performed on Gouy's balance and the diamagnetic correction were set by Pascal's constants. Thermo gravimetric test was performed underN2 with a heating rate 10 °C min-1 on Shimaduz corporation 60H analyzer. The values of absorbance of 5× 10-3 M of each complex were measured at various pH levels. The pH levels were checked by using a series of Britton universal buffers [12, 13, 16, 18, and 20]. PH measurements were made using HANNA 211 pH meter at 298 K.

2.4 Quantum Mechanics Modeling of the Ligands and Complexes Structures

Theoretical calculations for 2-[(4-Nitro-benzylidene)-amino]-pyridin-3-ol ligand (ahpnb) were performed using DFT approximation methods. Geometry optimization calculations were done using B3LYP functional and basis set LANL2DZ with operative core potential (ECP) [3, 12, 13, 21]. Gaussian 03 program package was used for all calculations. Calculations were performed for ahpnb ligand, as well as its Fe(II), Co(II), and Cu(II) complexes [3, 12, 13, 22].

2.5 In Vitro Antibacterial and Antifungal Bioassay

The in vitro biological activity of the tested Schiff bases and their metal complexes were tested against the bacteria [Escherichia coli, *Micrococcus luteus* and Serratiamarcescence] by the disc spread method using nutrient agar as the environment and Ofloxacin as control. The anti fungalactions of the compounds were also tested by the well diffusion route against the fungi [*Aspergillusflavus, Getrichm candidum and Fusarium oxysporum*] on potato dextrose agar as the medium and Fluconazolas the control. The complexes was fluxed in DMSO and the solutions of concentrations 10 and 20(mg/ml) were prepared separately. In a typical route, a well was made on the agar medium inoculated with micro-organism. The well was full with the experiment sol using a micropipette and the plate was incubated 24 h at 37 °C for the bacteria or72 h at 32 °C for the fungus organism. After incubation, the diameter of the obvious zone of inhibition surrounding the sample was taken as a measure of the inhibitory force of the sample against the particular test organism [3,12, 13, 16,18,24].

2.6 DNA Binding Study

All the tests involving the reaction of the complexes with DNA were carried out in Tris–HCl buffer (50 mM, pH7.2). CT-DNA was refined by centrifugal dialysis beforeuse. A solution of calf thymus DNA in the buffer offered a ratioof UV absorption at 260 and 280 nm of about >1.85, indicatingthat the DNA was sufficiently free from protein pollution [2-5,12, 13, 16,18, 24]. The concentration of DNA was determined by monitoring the UV absorbance at 260 nm usingε260= 6600 mol-1cm2. The stock solution was saved at4°C and utilized within only one day.

2.6.1Electronic Spectra of Interaction with DNA

All the experiments including the interaction of the complexes with DNA were carried out in Tris–HCl buffer (47mM, pH=7.1). CT-DNA was purified by centrifugal dialysis before utilization. A sol of calf thymus DNA in the buffer donated a ratio of UV absorbance at 260 and 280 nm of about >1.86, explaining that the DNA was sufficiently free from protein impurities [16, 18, 24]. The concentration of DNA was determined by monitoring the UV absorbance at 260 nm using ε260= 6600 mol-1cm2. The stock solution was saved at 4°C and utilized within only one day. Spectrophotometeric titration experience was implemented by retention the metal complex concentration constant while changing the nucleic acid concentration in the interaction environment. The absorption due to free CT-DNA was eliminated by addition an equimolar CT-DNA to refined buffer solution in the reference compartment and the consequent spectra were resulted from the metal complexes and the DNA – metal complex assemblages. From the absorption data, the intrinsic binding constant (Kb) was calculated through plotting [DNA]/ (εa-εf) vs. [DNA] according to the following equation:

$$\frac{[DNA]}{(\varepsilon_a - \varepsilon_f)} = \frac{[DNA]}{(\varepsilon_b - \varepsilon_f)} + \frac{1}{[K_b(\varepsilon_b - \varepsilon_f)]}$$

where, [DNA] is the concentricity of DNA in base pairs, εa, ε_f and ε_b are the apparent, free and fully bound complex absorptivity coefficients, respectively. In particular, εf was evaluated from the calibration curve for the isolated metal complex; following the Beer's law. Ea was evaluated as the ratio between the estimated absorbance and the metal(II) complex concentration, A_{obs} /[complex]. The data were suited to the above equation with a slope equal to $1/(\varepsilon_b-\varepsilon_f)$ and y-intercept equal to $1/[Kb\ (\varepsilon_b-\varepsilon_f)]$ and Kb was obtained from the ratio of the slope to the intercept [2-5, 16, 18, 25]. The standard Gibbs free energy for DNA interaction was evaluated from the following relation [2-5, 26]:

$$\Delta G_b^{\neq} = -RT \ln K_b$$

2.6.2 Viscosity Experiments for Interaction of the Prepared Complexes with DNA

Viscosity measures were carried out utilizing an Oswald microviscometer, maintained at steady temperature at 25±1°C in thermostat. The fluidity times were registered for various concentrations of the complex (10–200μM), maintaining the concentration of DNA constant (200 μM). Mixing of the solution was achieved by bubbling the nitrogen vapor through the viscometer. The average value of the three measures was used to determine the viscosity of the samples. The buffer fluidity time in seconds was registered as t°. The relative viscosities for DNA in the presence (η) and disappearance (η°) of the compound were evaluated using the relation η = (t _ t°)/t°. Where, t is the observed fluidity time in seconds and the values of the relative viscosity (η/η°) were plotted versus 1/R (R= [DNA]/ [Complex]) [2-5, 27, 29].

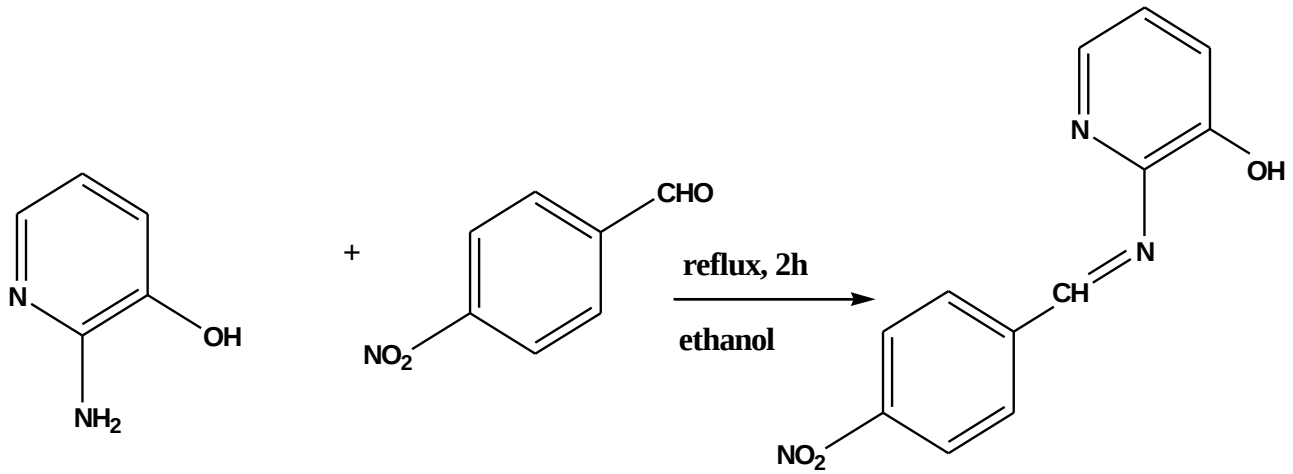

Scheme (1): synthesis of Schiff base ligand (ahpnb), where ahp=2-amino-3-hydroxypyridine and nb = 4-nitrobenzaldehyde.

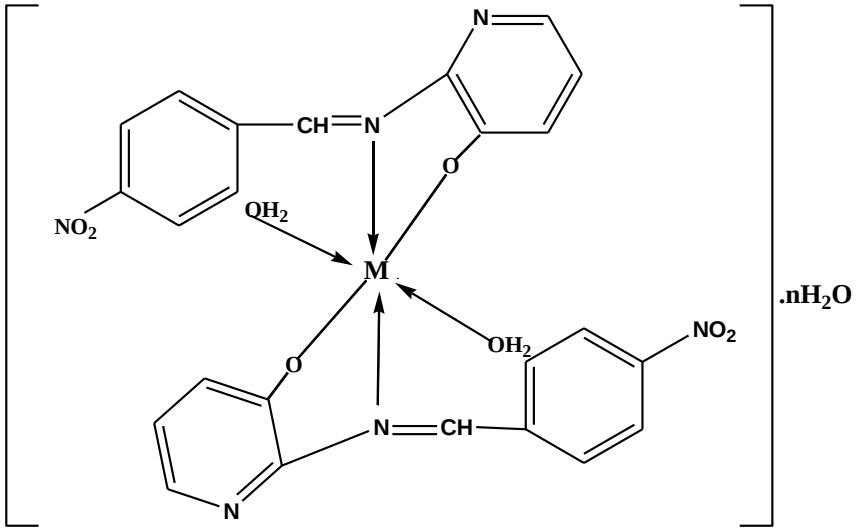

Scheme (2): The suggested structures of ahpnbFe, ahpnbCu, ahpnbNi, ahpnbCo complexes, ahpnbFe: n =1, ahpnbCu,ahpnbNi and ahpnbCo : n= 2.

2.6.3 Agarose gel Electrophoresis

The DNA binding products were tested by agarose gel electrophoresis method [3-5, 16, 28, 29]. The stock sol of complexes was prepared by dissolving 10 mg of the compounds in 10 ml of DMSO. The sample (25 μg/mL) was added to the isolated DNA of Calf-thymus (CT-DNA) and incubated for 2 h at 37 °C and then 20 μL of DNA sample (confused with bromophenol blue dye at a 1:1 ratio) was downloaded carefully into the electrophoresis chamber wells along with astandard DNA marker in TBE buffer (45mMTris base, pH 8.0; 1mM EDTA/1L) and finally loaded onto the agarose gel, then a constant electricity (40 V) was applied for about 45 min. Finally, the gel was eliminated and stained with 10 μg/ml of ethidium bromide for 10-20 min. The bands obtained was indicated under UV light using a transilluminator followed by photographed with DMC-LZ5 Lumix Digital Camera to determine the extent of DNA binding as compared with standard DNA marker.

3 Results and Discussion

3.1 Physicochemical Characteristics

All the metal complexes are tinted, solid, and steady at room temperature and non-hygroscopic matters. The Analytical and physicochemical data of ligand and their metal complexes are registered in (Table1). The metal complexes offer1:2 (metal-ligand) stoichiometry.

3.2Infrared Spectra

The distinctive IR frequencies of the ligand L1H and its complexes along with their assignments are listed in (Table 2). Bands due to –OH and –C=N are distinguishable and provide indication regarding the structure of the ligand and its bonding with metal [30-33]. A band at 1621 cm-1 in the ligand is assigned to −C=N stretching vibration. On coordination, this band is displaced to larger frequency. The negative shift of this band is obvious indication of the participation of the azomethine nitrogen atoms in complex formation [16,18, 28, 29, 33].
This is supported by the appearance of band at 656-685 cm-1 corresponding to the stretching vibration of M–N bond. Regions at 723-739 cm-1 correspond to M-O stretching vibrations. Band at 3475 cm-1 observed in the ligand is due to stretching vibrations of free –OH. In the complexes, the registered IR spectra of all the prepared complexes show broad band at 3480–3500 cm-1which have been as attributed to υ (OH) stretching vibration of hydrated water molecules, in accordance with the findings of the elemental analysis offered in table1. A band at 814–851 cm–1(OH rocking) suggests the presence of coordinated water in all four compounds. In the low frequency region, the band observed for Schiff base ligand showed an absorption band at 1288 cm-1 which can be resulted from the stretching vibration of the phenolic (C–O) group [34]. The shifting of that band to lower wave number values upon complex ation explains that the oxygen atoms of the phenolic groups are coordinated to the metal ion. The bands observed in the regions 3054–3090 cm-1 can be assigned to υ(C–H) aromatic stretching vibrations [28, 29].

3.3 ^{1}H-NMR Spectra

The ^{1}H-NMR spectra of the L_1H ligand shows the signal at 7.25-8.46 (m) δ for aromatic proton and 9.39 (s) δ for azomethine proton [35]. The peak at 6.41 (s) δ attributed to –OH group present in pyridine moiety, disappeared upon addition of D_2O [36].

3.4. Spectro Photometric Determination of the Stoichiometry of the Prepared Complexes

Stoichiometry of prepared complexes is determined using the two methods involving the use of spectrophotometry, namely, continuous-variations route (CVM), mole-ratio method (MRM)[28, 29,31-33]. Based on the methods used and the experimental results, the stoichiometry of the prepared complexes is 1:2. The curves of the continuous variation method (Figure.1) displayed maximum absorbance at mole fraction X_{ligand} = 0.65–0.7 explaining the formation of complexes with metal ion to ligand ratio 1:2. Moreover, the data obtained from applying the molar ratio route support the same metal ion to ligand ratio of the prepared complexes (Figure.2) [37].

3.5 Determination of the Apparent Formation Constants of the Prepared Complexes

The formation constants (K_f) of the studied Schiff base complexes formed in solution were gotten from the spectrophotometric measurements by applying the continuous variation method according to the following equation [28, 29, 38, 39]:

$$\mathbf{K}_{\mathrm{f}} = \frac{A / A_m}{4C_2[1-(A/A_m)]^3}$$

Where, $A_m$is the absorbance at the maximum creation of the complex, A is the arbitrary chosen absorbance values on either side of the absorption mountain col (pass) and C is the primary concentration of the metal. As mentioned in (Table 5), the obtained K_f values explain the great stability of the tested complexes. The values of K_f for the checked complexes increase in the following order: ahpnbFe> ahpnbNi>ahpnbCo> ahpnbCu. Moreover, the values of the constancy constant (pK) and Gibbs free energy ($\Delta G^{\neq}$) of the presented complexes are calculated. The negative values of Gibbs free energy indicate that the reaction is spontaneous and favorable. The pH-profile (absorbance vs. pH) found in (Figure.3) showed typical dissociation curves and a great stability Ph range (4–10) of the studied complexes. This refers to that the formation of the complex greatly stabilizes the Schiff base ligands. Consequently, the suitable pH range for the different applications of the prepared complexes is from pH =4 to pH = 10.According to the results of elemental analysis, molar conductance, magnetic measures, infrared and electronic spectra, the suggested composition of the complexes.

3.6 Electronic Spectra

The electronic absorption spectra are often very important in the evaluation of results furnished by other methods of structural check. The electronic spectral measures were used for assigning the stereochemistries of metal ions in the complexes based on the sites and number of *d–d* transition peaks [39].The electronic absorption spectra of ligands and their complexes were registered at the wavelength range 800–200 nm and at 298 K. The ligand exhibits absorption bands in UV–Vis region around 344 nm which is assigned to n→π*transition originating from the imine function of the Schiff base ligand and ab and in 220 nm due to aromatic rings of ligand. The absorption bands of complexes at λ_{max} = 350-453 nm is assigned to charge transfer with in Schiff

base ligands. [41]. Furthermore, A long and a broad band lying in the region 416–506 nm. This band could be mainly attributed to the d → d transition in the octahedral structure of the prepared complexes [42].

3.7 Thermal Analysis

The thermogram of Cu(II), Fe(III), Co(II) and Ni(II) complexes confirms the presence two coordinated water molecules. Hence from TGA it is clear that the complex under study includes two coordinated water molecules which are coordinated to central metal ion [28, 29]. The thermal behavior of the metal complexes showed that the hydrous complexes lose water molecules of hydration in the first step; then lose coordinated water molecules with decomposition of the ligand molecules in the subsequent steps as shown in (Table 3).

The ahpnbCu, ahpnbCo, ahpnbNi and ahpnbFe complexes have weight losses of 6.55, 5.80, 5.60 and 3.05 % respectively, which are due to removal of water molecules of hydration. The weight losses of 12.56, 50.21 and 19.66 % corresponding to the elimination of the remaining thermally degradable part of the complex at temperature range 165.7-409.3 °C with respect to ahpnbCu complex. The weight losses of 12.56, 50.21 and 19.66 % corresponding to the elimination of the remaining thermally degradable part of the complex at temperature range 165.7-409.3 °C with respect to ahpnbCu complex. The weight losses of 52.60, 31.89 and 19.66 % corresponding to the elimination of the remaining thermally degradable part of the complex at temperature range 103.2-483.0 °C with respect to ahpnbCo complex. The weight losses of 30.36 and 54.58 % corresponding to the elimination of the remaining thermally degradable part of the complex at temperature range 100.2-508.5 °C with respect to ahpnbNi complex. The weight losses of 49.48 and 37.44 % corresponding to the elimination of the remaining thermally degradable part of the complex at temperature range 176.1-490.9 °C with respect to ahpnbFe complex. The final product is metal.

3.7.1 Kinetic Aspects

The thermodynamic parameters of the degradation processes of the complexes were calculated using the Coasts- Redfern equation [28, 29]:

$$\log\left[\frac{\log(w_\infty - w))}{T^2}\right] = \log\left[\frac{AR}{\phi E*}\left(1-\frac{2RT}{E*}\right)\right] - \frac{E*}{2.303RT} \quad (4)$$

Where W∞ is the mass loss at the end of the decomposition reaction. W is the mass perishing up to temperature T, R is the gas constant and ϕ is the warming rate. Since 1-2RT/E* ≈1, the plot of the left side of equation against 1/T would give a straight line. E^* was then estimated to form the slope and the Arrhenius constant, A, was gained from the intercept. The other kinetic parameters; the entropy of energizing (S^*), enthalpy of activation (H^*) and the free energy variance of activation (G^*) were calculated utilizing the following equations:

$$S^* = 2.303R \log \frac{Ah}{kT} \quad (5)$$

$$H^* = E^* - RT \quad (6)$$

$$G^* = H^* - TS^* \quad (7)$$

Where (k) and (h) are Boltzmann's and Plank's invariables, respectively. The Kinetic parameters are shown in (Table 4).It is shown that G* values increase due to increasing temperature. The positive values of H* explain that degradation processes are endothermic. In most thermal steps, S* values are negative suggesting a degradation via abnormal pathway at those steps and the degradation processes are unfavorable. The negative activation entropy value explains that the activated complexes were more ordered than the reactant and that the reactions were dilatory. The more ordered nature was attributed to the polarization of bonds in the activated state, which might occur through charge transfer electronic transitions. Finally, positive values were found for H* and G* respectively representing endothermic character for all thermal steps.

3.8 Magnetic Moment Measurements

The paramagnetic compounds have affinity to magnetic field while the diamagnetic compounds repelled in a magnetic field. For paramagnetic materials, the flux is greater within the matter than it would be in vacuum. Therefore, paramagnetic materials will have positive susceptibilities. Thus, the magnetic susceptibility measures provide information regarding the geometric composition of the complexes. Magnetic susceptibility measures indicated that the prepared complexes have paramagnetic character [28,29].

3.9 Modeling of Metal (II) 2-[(4-Nitro-Benzylidene)-Amino]-Pyridin-3-ol Complexes

Optimization of 2-[(4-Nitro-benzylidene)-amino]-pyridin-3-ol (ahpnb) structure showed that it had a planner geometry, where the Phenolic oxygen, azomethine nitrogen

were facing each other with dihedral angle equal to 0.0°. This orientation enables ahpnb to coordinate with metal ions forming aromatic-like structure. (Figure 4) show the optimized structure of Fe(II), Co(II) and Cu(II) complexes. Optimization showed that all complexes had octahedral coordination with the ligand. More specifically the metal was bounded to the ligand with 1:2 ratio. The ligand acted as di-dentate through, the hydroxyl, and azomethine groups. The octahedral geometry was fulfilled by two water molecules. The average bond lengths for the (M- ahpnb) bonds were found to be 1.91Å and 2.03Å for M-N and M-Orespectively. For the additional water molecules had bond distances 2.01 Å for M-OH_2. The key factor for the high stability of the formed complexes is due to the formation of aromatic five rings between the M^{2+} center and the ligand molecule. The legand molecules were oriented in parallel plane with dihedral angle of 176.5°, and the estimated dihedral angle with the coordinated water was 84.3°. The relative stability of the calculated complexes as well as the relative chemical reactivity was estimated by calculating the global chemical reactivity descriptors (energy band gap, chemical hardness, electronic chemical potential (strain) and electrophilicity) [43, 44]. The physical meaning of these descriptors is defined as follow: Chemical hardness (η) in a molecule refers to the resistance to change in the electron division or charge transfer. The electronic chemical potential (μ) is a measure of electro negativity of the molecule. The electro philicity index (ω) measures the propensity or the capacity of a species to accept electrons. Table 6abridged the computed chemical descriptors for all models under investigation. Chemical hardness (η) is attached with the stability and reactivity of a chemical array. On the basis of frontier molecular orbitals, chemical hardness matches the energy gap between HOMO and LUMO. The greater the energy gap, the harder and more stable/less reactive the molecule. Among the calculated complexes, [Co $(ahpnb)_2(H_2O)_2$] has the largest η while [$Fe(ahpnb)_2(H_2O)_2$] has the lowest η. These results agree with the experimentally calculated stability constant. The insignificant difference between η values reflects their similar colors as well as the limited distinction between the observed λ_{max} for complexes.

3.10 Antimicrobial Activity

The antibacterial potency of the Schiff base and its metal complexes on bacteria organisms*[Escherichia coli, Micrococcus luteu* sand *Serratiamarcescence]* and versus the fungi *[Aspergillusflavus, Getrichm candidum and Fusarium oxysporum]*.was tested in order to assess their potential antimicrobial agents. The biological dynamism of the Schiff base ligand and its metal complexes were also matched with **Ofloxacin** (Antibacterial agent) and **Fluconazol** (Antifungousagent). The data are presented in Table (7, 8) and Figure (5, 6). According to the data it can be seen that the ligand show weak biological activity, while all the complexes showed strong activity against bacteria and fungi [45]. This means that the potency of the newly prepared Schiff base versus different microorganisms is improved with chelation with different biological active metals. The minimum inhibitory concentration (MIC) was estimated by serial dilution technique and reported in Table (9, 10).A comparative study of the ligand and its complexes, indicates that the complexes exhibit greater antimicrobial potency than the free ligand. Such increased activity of the complexes can be explained on the basis of Overtone's concept and Tweedy's chelation hypothesis. According to Overtone's notion of cell permeability, the lipid membrane that surrounds the cell favors the bypassing of only the lipid-soluble materialsdue to which liposolubility is an serious factor, which controls the antimicrobial activity. On chelation, the polarity of the metal ion will be decreased to a greater extent due to the interfere of the ligand orbital and partial sharing of the positive charge of the metal ion with donor groups. Further, it augments the delocalization of π-electrons over the whole chelate ring and improves the lipophilicity of the complexes [16, 18, 28, 29,45]. This rise of lipophilicity improves the penetration of the complexes into lipid membranes and blocking of the metal bindingpositions in the enzymes of microorganisms. These complexes also discomfort the respiration process of the cell and thus block the formation of the proteins that restricts further growth of the organism.

3.11 DNA Binding Activity

3.11.1 Electronic Spectra of Interaction with DNA

In general, the hyperchromism and hypochromism were regarded as spectral lineaments for DNA double-helix structural variance when DNA reacted with other molecules. The hyper chromism arises from the breakage of the DNA duplex secondary structure; the hypochromismsets from the stability of the DNA duplex by either the intercalation binding pattern or the electrostatic effect of small molecules [46].All the compounds show decrease in absorbance indicates that there is binding to CT DNA via an intercalative mode which are shown in (Figure.7).Binding constant values is more comparable with typical known intercalators (EB-DNA, 0.33×10^5 L mol^{-1}). The spectral parameters for the DNA interaction with the prepared complexes are shown in (Table 11). It can be known from the high percent of hyperchromicity that the high strength binding of the prepared complexes with DNA. The tested complexes could bind to DNA via an intercalative mode with the sequence: ahpnbFe> ahpnbCu> ahpnbNi> ahpnbCo. The results revealed that the difference of the metal might lead to clear difference of DNA binding abilities of the complexes.

3.11.2 Viscosity Measurements

Optical photophysical studies are not enough to explain a connection between DNA and the complex. To further make obvious the interaction between the complex and CT DNA, viscosity measurements were implemented for all complexes. Hydrodynamic measurements that are sensitive to length vary (i.e. viscosity and sedimentation) areconsidered as the least mystic and the mostcritical tests of a binding model in solution in the obscurity of crystallographic structural data [16, 18, 28, 29]. A classical intercalation modeldemands that the DNA helix must lengthen as base pairs are segregated to adjust the binding complexes, leading to the increase of DNA viscosity, as for the patterns of the known DNA intercalators [47]. On the contrary, a partial and/or non-classical intercalation of the complex could kink the DNA helix, decreasing its viscosity concomitantly. Moreover, some complexes such as $[Ru(bpy)_3]^{2+}$, which react with DNA through an electrostatic binding mode, have no influence on DNA viscosity. The effects of whole the compounds on the viscosity of CT DNA are shown in (Figure.8). The viscosity measurements clearly explained that all the compounds can intercalate between adjacent DNA base pairs, causing a boost in the DNA helix and thus raising the viscosity of DNA with an increasing concentration of the complexes. We find that the metal complexes can bind to CTDNA via an intercalative mode.

3.11.3 Gel Electrophoresis

The metal (II) complexes were subjected to their DNA binding activity by gel electrophoresis method. The Ni(II) (lane 1), Cu(II) (lane 2), Co(II) (lane 3) and Fe(II) (lane 4) complexes show partial DNA binding as presented in (Figure.9). A difference in the bands of complexes (lanes 1-4) was observed as compared to that of control Calf-thymus DNA. The binding efficiency of the complexes compared with that of the control is due to their great DNA-binding ability [48]. Hence it was accomplished that the control DNA alone does not show any apparent binding, whereas its complexes show promising activity, along with this it explain the fundamental role of metal ions in these isolated DNA binding reactions. However, the nature of the active intermediates involved in the DNA binding by the complexes is not clear. Thus from the above, it was clear explained that as the complexes was observed to cleave the DNA, therefore inhibits the outgrowth of the pathogenic organism by cleaving the genome [49].The experimental results illustrated that the investigated complexes could be bound to DNA via intercalative pattern and showed a different DNA binding activity according to the sequence: ahpnbFe> ahpnbCu> ahpnbNi> ahpnbCo.

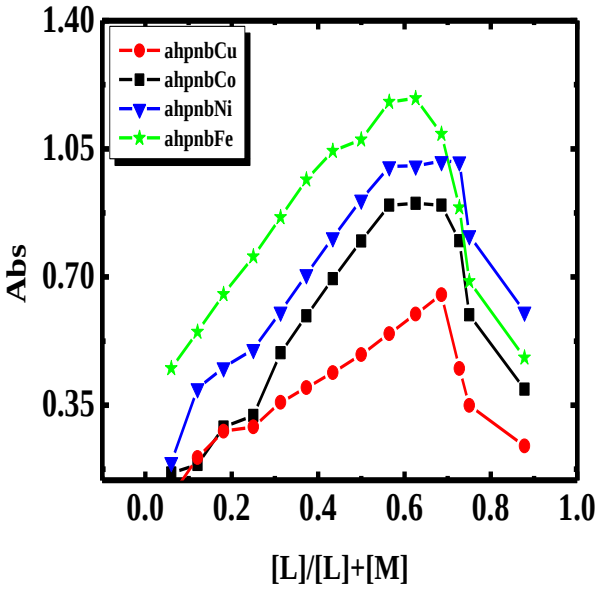

Fig.1: Continuous variation plots for the prepared complexes in aqueous-alcoholic mixture at [complex] = 1 $\times 10^{-3}$M and 298 K.

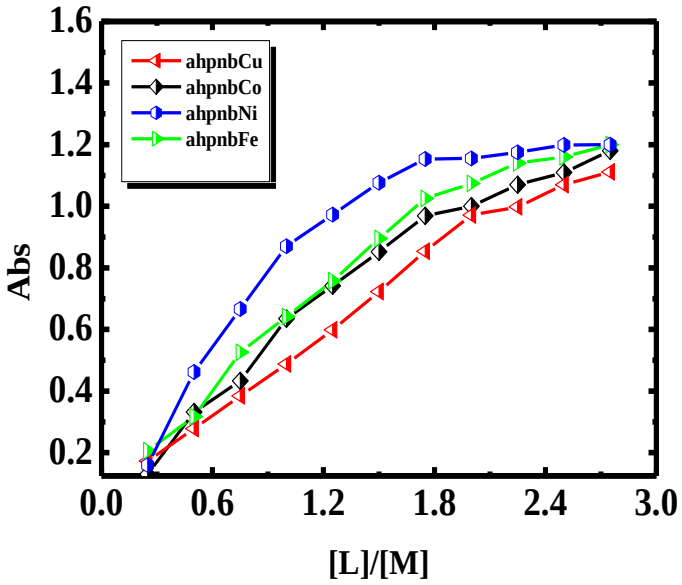

Fig. 2: Molar ratio plots for the studied complexes in aqueous- alcoholic mixture [M]=[L1H]=1×10-3 and 298 K.

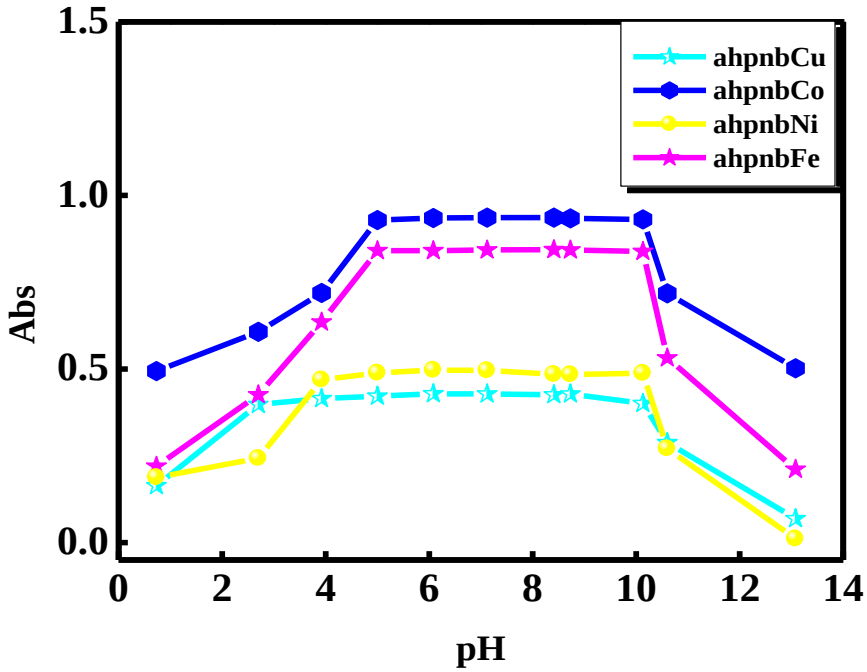

Fig. 3: Dissociation curves of the prepared complexes in aqueous alcohol mixture at [complex] = 1 $\times 10^{-3}$ M and298 K.

Table 1: The Analytical and physical data of ligand and Its Metal complexes

Compound	Color	(m.p) and Decomposition point	M.wt	Elemental Analysis found(calculated)			Conductance Λm ($\Omega^{-1}cm^2$ mol^{-1})	μ_{eff} B.M.
				C	H	N		
L_1H	Brown	245	243	59.25 (59.21)	3.70 (3.74)	17.28 (17.32)	6.08	-
$[Cu(L_1)_2(H_2O)_2].2H_2O$	Black	>300	619.5	46.48 (46.35)	3.87 (3.79)	13.55 13.49)(	8.87	2.5
$[Co(L_1)_2(H_2O)_2].2H_2O$	Black	>300	614.9	46.83 (46.78)	3.90 (3.85)	13.66 13.52)(	7.48	3.81
$[Ni(L_1)_2(H_2O)_2].2H_2O$	Brown	>300	614.7	46.85 (46.83)	3.90 (3.88)	13.66 (13.69)	2.38	3.11
$[Fe(L_1)_2(H_2O)_2].H_2O$	Brown	>300	593.8	48.50 (48.59)	3.70 (3.66)	14.14 14.29)(	12.97	5.24

Model	Optimized Structure
ahpnb Ligand	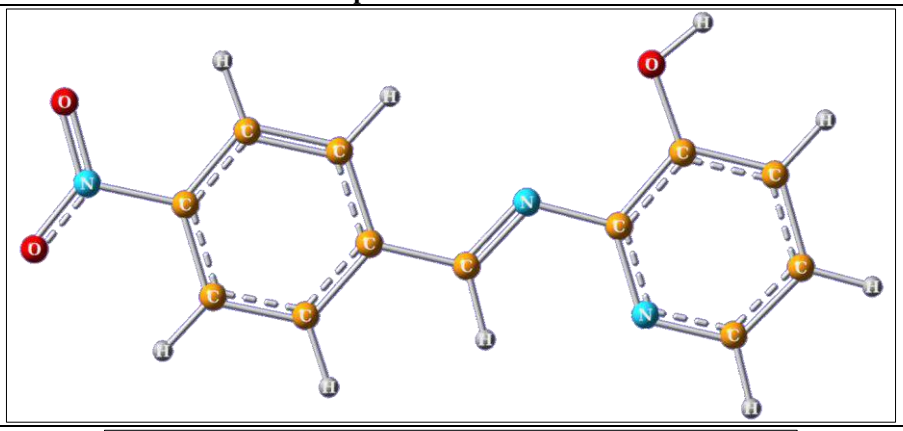
ahpnbFe	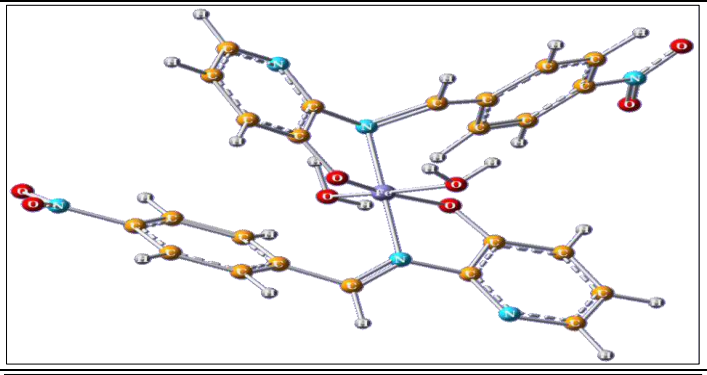
AhpnbCo	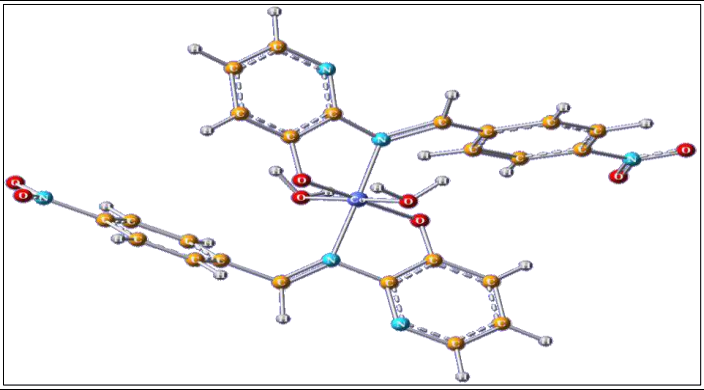
ahpnbCu	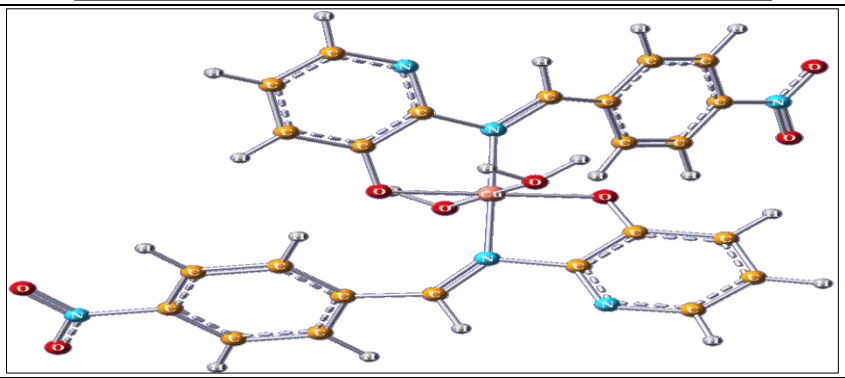

Fig. 4: Optimized structures of the ahpnbmolecule and Fe(II), Co(II), Cu(II) complex models calculatedat DFT approximation method

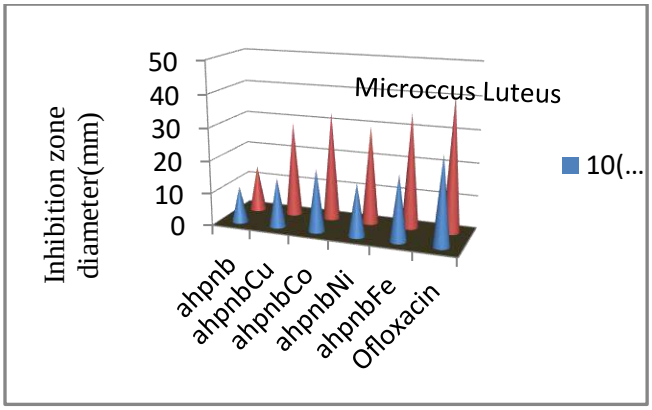

Fig.5: Zone of inhibition against Microccus luteus (bacteria) by prepared complexes.

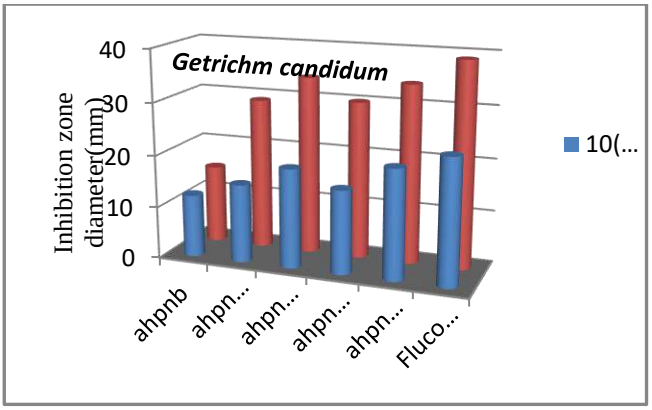

Fig.6: Zone of inhibition against Getrichm candidum (fungi) by prepared the complexes.

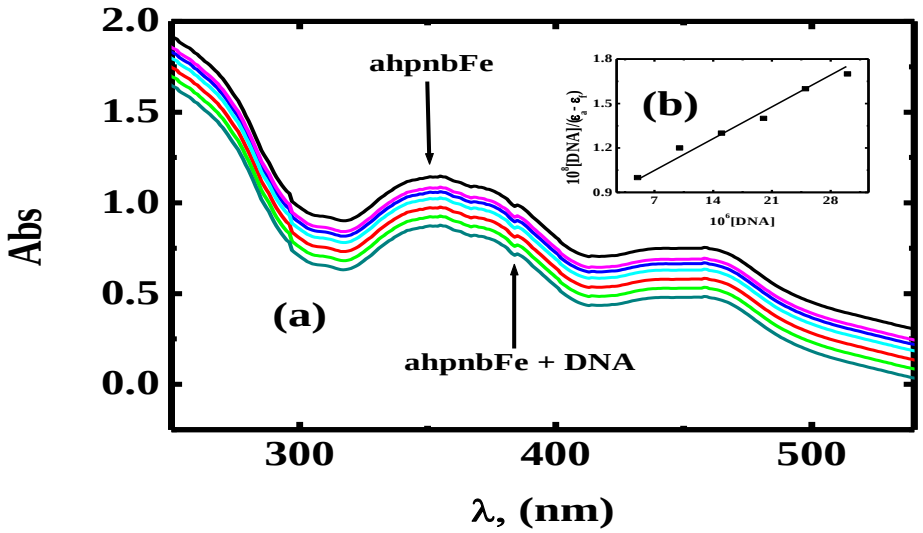

Figure.7: (a) Spectrophotometeric titration of ahpnbFe complex(10-3 M) in 0.01 M Tris buffer (pH= 7.5, 25oC) with CT DNA(from top to bottom, 0–40 µM DNA, at 5µM intervals). (b) Plotof [DNA]/(εa-εf) vs. [DNA] for the titration of DNA with ahpnbFe complex.

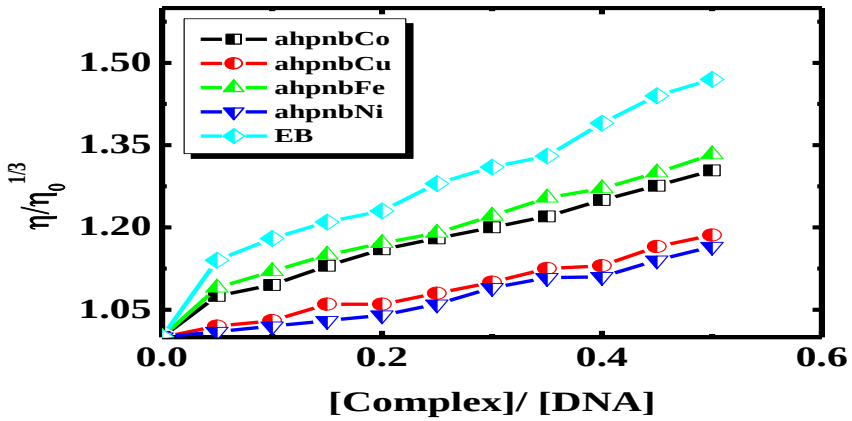

Fig. 8: The effect of increasing the amount of the synthesized complexes on the relative viscosities of DNA at [DNA] =0.5 mM,[complex] =25–250 µM and 298 K.

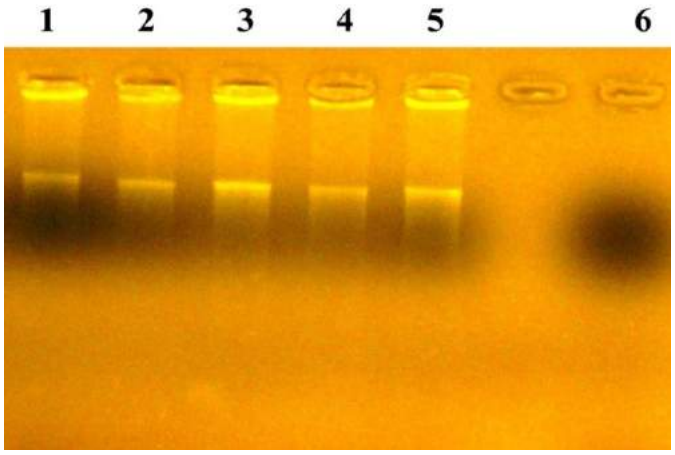

Fig. 9: DNA binding study Calf-thymus (CT) -DNA with Cu (II), Ni (II), Co (II) and Fe (II) Complexes. Lane1: Ni(II) ; Lane 2: Cu (II) ; Lane 3: Co (II) ; Lane 4: Fe (II); Lane 5: Control DNA ; Lane 6: Blank.

Table 2: Infrared spectral bands of Schiff base ligand and its complexes.

Compound	υ (OH/ H_2O)	(CH_{aro})υ	(C=N)υ	υ(C-O) phenolic	(H_2O)υ Coordinat	(M-O)υ	(M-N)υ
L_1H	3475(w)	3100(w)	1621(s)	1288(m)	-	-	-
$[Co(L_1)_2(H_2O)_2].2H2O$	3490(w)	3079(w)	1615(s)	1286(w)	814(w)	723(w)	656(w)
$[Cu(L_1)_2(H_2O)_2].2H2O$	3500(w)	3054(w)	1620(s)	1285(m)	848(m)	739(m)	685(m)
$[Fe(L_1)_2(H_2O)_2].H_2O$	3495(w)	3090(w)	1590(s)	1255(w)	850 (w)	736(m)	659(w)
$[Ni(L_1)_2(H_2O)_2].2H_2O$	3480(w)	3077(w)	1597(s)	1251(m)	851(m)	739(w)	661(w)

s=Strong, m= medium, w= weak.

Table 3: Thermal Analysis data for metal complexes.

Complex	Degradation Temperature °C	Lost fragment	Weight Loss%	
			theoritical	found
$[Cu(L_1)_2(H_2O)_2].2H_2O$	34-165	$2H_2O$	5.81	6.55
	165-243	$2H_2O + NO_2$	13.23	12.56
	243-310	$C_{17}H_{11}N_4O_3$	51.49	50.21
	310-409	C_7H_5NO	19.20	19.66
	>409	Cu	10.27	11.02
$[Co(L_1)_2(H_2O)_2].2H_2O$	33-103	$2H_2O$	5.85	5.80
	103-292	$2H_2O + C_{12}H_8N_4O_5$	52.69	52.60
	292-483	$C_{12}H_8N_2O$	31.87	31.89
	>483	Co	9.60	9.71
$[Ni(L_1)_2(H_2O)_2].2H_2O$	33-100	$2H_2O$	5.85	5.60
	100-258	$2H_2O + C_7H_5N_2O_2$	30.09	30.36
	258-508	$C_{17}H_{11}N_4O_4$	54.49	54.58
	>508	Ni	9.57	9.46
$[Fe(L_1)_2(H_2O)_2]. H_2O$	34-176	H_2O	3.03	3.05
	176-345	$2H_2O + C_{12}H_8N_3O_4$	49.51	49.48
	345-490	$C_{12}H_8N_3O_2$	38.05	37.44
	>490	Fe	9.42	10.03

Table 4: Kinetic parameters of the prepared metal complexes.

Complex	T (°C)	H* (KJ.mol^{-1})	S* (Jmol^{-1}K^{-1})	G* (KJ.mol^{-1})
[CuL$_1$H$_2$O].H$_2$O	145	0.52	-234.34	21.55
	265	1.77	- 242.67	41.98
	411	3.09	- 244.65	56,99
	640	3.59	-248.76	71.66
[CoL$_1$(H$_2$O)$_3$].H$_2$O	143	0.46	- 235.43	17.56
	218	1.88	- 245.52	35.55
	376	2.41	- 248.42	55.87
	498	3.45	-251.78	69.42
[NiL$_1$(H$_2$O)$_3$].H$_2$O	157	0.50	-233.54	11.55
	266	1.56	- 245.50	29.65
	342	2.39	- 249.55	42.89
	468	-3.33	-234.34	63.86

Table5: The formation constant (Kf), stability constant (pK) and Gibbs free energy (ΔG≠) values of the synthesized complexes in aqueous-ethanol at 298 K.

Complex	Type of complex	K_f	-log K_f	$\Delta G^{\neq}$ kJ mol^{-1}
[Cu(L$_1$)$_2$(H$_2$O)$_2$].2H$_2$O	**1:2**	**$3.62 \pm 0.02 \times 10^{10}$**	**10.55**	**-60.20**
[Co(L$_1$)$_2$(H$_2$O)$_2$].2H$_2$O	**1:2**	**$2.75 \pm 0.02 \times 10^{11}$**	**11.43**	**-65.22**
[Ni(L$_1$)$_2$(H$_2$O)$_2$].2H$_2$O	**1:2**	**$1.12 \pm 0.02 \times 10^{11}$**	**11.04**	**-63.00**
[Fe(L$_1$)$_2$(H$_2$O)$_2$].H$_2$O	**1:2**	**$2.47 \pm 0.02 \times 10^{11}$**	**11.39**	**-64.96**

Table 6: Calculated HOMO, LUMO, energy gap (Δ*E*), chemical hardness (η), electronic chemical potential (μ) and electrophilicity (ω) of the ligand and its corresponding Fe(II), Co(II) and Cu(II) complexes. All values were calculated in eV unit.

Compound	HOMO (ev)	LUMO (ev)	ΔE (ev)	η (ev)	μ (ev)	ω (ev)
ahpnb	-6.15	-2.32	3.83	1.92	-4.24	4.68
[ahpnbCu]	-4.08	-1.61	2.47	1.24	-2.85	3.28
[ahpnbCo]	-12.82	-10.42	2.40	1.20	-11.62	56.26
[ahpnbFe]	-12.90	-11.31	1.59	0.80	-12.11	92.16

Table 7: Results of antibacterial activity of the prepared ligand and itscomplexes in DMSO

Compounds	**Inhibition zone (mm)**					
	***Serratia Marcescence* (-ve)**		***Escherichia coli* (-ve)**		***Microccus Luteus* (+ve)**	
Conc. (mg/ml)	**10**	**20**	**10**	**20**	**10**	**20**
ahpnb	**6**	**10**	**5**	**8**	**11**	**14**
ahpnbCo	**14**	**23**	**11**	**17**	**19**	**33**
ahpnbCu	**11**	**19**	**8**	**14**	**15**	**29**
ahpnbFe	**16**	**24**	**12**	**19**	**20**	**35**
ahpnbNi	**11**	**20**	**9**	**14**	**16**	**30**
Ofloxacin	**22**	**31**	**17**	**24**	**27**	**41**

Table8: Results of antifungal activity of the prepared ligand and itscomplexes in DMSO

Compounds	**Inhibition zone (mm)**					
	Aspergillus flavus		***Getrichm candidum***		***Fusarium oxysporum***	
Conc. (mg/ml)	**10**	**20**	**10**	**20**	**10**	**20**
ahpnb	**4**	**7**	**12**	**15**	**6**	**10**
ahpnbCo	**11**	**17**	**19**	**34**	**15**	**22**
ahpnbCu	**8**	**14**	**15**	**29**	**12**	**22**
ahpnbFe	**12**	**19**	**21**	**34**	**17**	**24**
ahpnbNi	**9**	**14**	**16**	**30**	**15**	**24**
Fluconazol	**15**	**24**	**24**	**39**	**21**	**31**

Table 9: Results ofMinimum inhibition concentration (MIC)of the prepared Schiff base ligand and its complexesagainst different strains of bacteria.

	Minimum inhibition concentration(MIC) (mg/ml)		
Bacteria / Compounds	***Serratia Marcescence***	***Escherichia coli***	***Microccus Luteus***
ahpnb	**8**	**6**	**3**
ahpnbCo	**4**	**5**	**3**
ahpnbCu	**7**	**8**	**7**
ahpnbFe	**9**	**7**	**2**
ahpnbNi	**5**	**8**	**3**

Table 10: Results ofMinimum inhibition concentration(MIC)of the prepared Schiff base ligand and its complexesagainst different strains of fungi.

	Minimum inhibition concentration(MIC) (mg/ml)		
Fungi / Compounds	*Aspergillus flavus*	*Getrichm candidum*	*Fusarium oxysporum*
ahpnb	**7**	**9**	**8**
ahpnbCo	**3**	**6**	**9**
ahpnbCu	**4**	**3**	**8**
ahpnbFe	**5**	**2**	**7**
ahpnbNi	**8**	**3**	**5**

Table 11: Spectral parameters for DNA interaction with the synthesized complexes.

Complex	λ_{max} Free (nm)	λ_{max} Bound (nm)	Δn (nm)	Chromism (%)[a]	Type of Chromism	Binding Constant $K_b \times 10^6$ $mol^{-1}dm^3$	$\Delta G^{\neq}$ KJ mol^{-1}
$[Cu(L_1)_2(H_2O)_2].2H_2O$	506 301	497 302	9 1	52.1 50.6	Hypo Hypo	0.04 ± 0.02	-26.24
$[Co(L_1)_2(H_2O)_2].2H_2O$	423 226	426 225	3 1	41.3 21.6	Hypo Hypo	0.03 ± 0.02	-25.52
$[Ni(L_1)_2(H_2O)_2].2H_2O$	416 350	424 353	8 3	38.3 38.2	Hypo Hypo	0.06 ± 0.02	-27.40
$[Fe(L_1)_2(H_2O)_2].H_2O$	462 353	459 355	3 2	35.1 23.6	Hypo Hypo	0.03 ± 0.02	-25.53

[a]**Chromism (%) = [(Abs $_{free}$- Abs $_{bound}$) /Abs $_{free}$]**

4 Conclusions

The Schiff base was derived by the condensation of 4-nitrobenzaldehyde with 3-methoxysalicylaldehyde. The prepared transition metal complexes have been found to be of the type $[M(L_1)_2(H_2O)_2].nH_2O$. The analytical data indicate that the complexes have 1:2 (metal: ligand) stoichiometry. Conductivity measure shows their non-electrolytic nature. L_1H ligand coordinates with the metal ions through the pyridyl-O and azomethine-N. The ^{1}H-NMR data suggest that the Schiff base ligand deprotonated after complexation. Thermal data show degradation pattern of the complexes. Thermo gravimetric survey of the complexes also helpedto characterize the complexes. Very good antimicrobial activity of the selected complexes was found against examined organisms. The DNA interaction of these complexes was tested by using gel electrophoresis and viscosity measures. The experimental findings showed that the investigated complexes could bind to DNA via intercalative mode.

Acknowledgment

The authors are thanks to Dr. Mohamed Ismail for doing theoretical calculations.

References

[1] F. P. Dwyer and D. P. Mellor, Chelating Agents and Metal Chelates, Academic Press, New York, NY, USA, 1964.

[2] A.M. Abu-Dief, R. Díaz-Torres, E.C. Sañudo, L.H. Abdel-Rahman, N.A. Alcalde,

Polyhedron., **64,** 203−208(2013).

[3] L. H. Abdel-Rahman, R. M. El-Khatib, L. A. E. Nassr, Ahmed M. Abu-Dief, M. Ismail, A. A. Seleem, SpectrochimicaActa Part A: Molecular and Biomolecular Spectroscopy., **117** , 366(2014).

[4] L. H. Abdel-Rahman, A. M, Abu-Dief, R. M. El-Khatib, S. M. Abdel-Fatah, J. Photochem. Photobio., B. **162**, (2016) 298–308.

[5] L. H. Abdel-Rahman, A. M. Abu-Dief, M., Ismael, M. A. A.,

Mohamed, N. A. Hashem, J. Mol. Struct. **1103,** 232 – 244(2016).

[6] S. Malik, S. Ghosh, and L. Mitu, Journal of the Serbian Chemical Society., **76(10)**, 1387–1394(2011).

[7] A. M. Abu-Dief and L. A. E. Nassr,J. Iran. Chem. Soc., **12,** 943-955(2015).

[8] L. H. Abdel-Rahman, A. M. Abu-Dief, S. K. Hamdan, A. A. Seleem, Int. J. Nano. Chim., **1**, 65 – 77(2015).

[9] Laila H. Abdel-Rahman, Ahmed M. Abu‐Dief, MaramBasha, Azza A. Hassan Abdel-Mawgoud, ApplOrganometal Chem. 2017;e3750.

[10] L.H. Abdel-Rahman, R.M. El-Khatib, A.M. Abu-Dief, S.M. Abdel-Fatah and A.A. Sleem, Int. J. Nano.Chem., **2,** 83-91(2016).

[11] K. Shivakumar, Shashidhar, P. V. Reddy, and M. B. Halli, Journal of Coordination Chemistry., **61(14)**, 2274–2287, 2008.

[12] Ahmed M. Abu-Dief, Ibrahim M.A. Mohamed, J. Basic Appl. Sci., **4**, 119−133(2015).

[13] Laila H. Abdel-Rahman, Nabawia M. Ismail, Mohamed Ismael, Ahmed M. Abu-Dief, Ebtehal Abdel-Hameed Ahmed, J. Mol. Struct., **1134**, 851-862(2017).

[14] K. R. Joshi, J. H. Pandya, and A. J. Rojivadiya, ICAIJ., **4**, 110–114(2009).

[15] K. S. Abou-Melha and H. Faruk, Journal of Coordination Chemistry., 61(12), 1862–1874(2008).

[16] L. H. Abdel-Rahman, A. M. Abu-Dief, E. F. Newair, S. K. Hamdan, J. Photochem. Photobiol. B., **160**, 18–3(2016).

[17] M. Sondhi, M. Dinodia, and A. Kumar, Bioorganic and Medicinal Chemistry., **14(13)**, 4657–4663(2006).

[18] Laila H. Abdel-Rahman, Ahmed M. Abu-Dief, Rafat M. El-Khatib, ShimaaMahdy Abdel-Fatah, Bioorganic Chemistry., **69**, 140−152(2016).

[19] Raman, L. Mitu, A. Sakthivel, and M. S. S. Pandi, Journal of the Iranian Chemical Society., **6(4)**, 738–748(2009).

[20] Britton, H.T.S.,Hydrogen Ions, third ed. Chapman and Hall,London, UK, 1952.

[21] P. J. Hay, W. R. Wadt, J. Chem. Phys., **82**, 270(1985).

[22] M. J. Frisch, G. W.Trucks, H. B. Schlegel, G. E. Scuseria, M. A. Robb, J. R. Cheeseman, et al. Gaussian 03, Revision of C.01. Wallingford CT: Gaussian Inc.; 2004.

[23] Laila H. Abdel-Rahman, Ahmed M. Abu‐Dief, Azza A. Hassan Abdel-Mawgoud, Journal of King Saud University −Science(2017), http://dx.doi.org/10.1016/j.jksus.2017.05.011

[24] J. G. Chen, X. Qiao, Y. C. Gao, et al, Journal of Inorganic Biochemistry., **109**, 90–96(2012).

[25] K. S. Prasad, L. S. Kumar, S. C. Shekar, M. Prasad, and H. D. Revanasiddappa, Chemical Sciences Journal., **(12)**, 1–10(2011).

[26] P. Jogi, M. Padmaja, K. V. T. S. Pavan Kumar, and C. Gyanakumari, Journal of Chemical and Pharmaceutical Research., **4(2)**, 1389–1397(2012).

[27] Laila H. Abdel-Rahman, Ahmed M. Abu‐Dief, Moustafa O. Aboelez,Azza A. Hassan Abdel-Mawgoud, Journal of Photochemistry & Photobiology, B: Biology., **170** 271–285(2017) .

[28] Laila H. Abdel-Rahman, Ahmed M. Abu‐Dief, H. Mustafa, Azza A. Hassan Abdel-Mawgoud, Arabian Journal of Chemistry (2017), http://dx.doi.org/10.1016/j.arabjc.2017.07.007

[29] Ahmed M. Abu-Dief, Mohammed S.M. Abdelbaky, SantigoGarcía-Granda, Acta, Cryst E.,**71**, 496−497(2015).

[30] Hany M. Abd El-Lateef, Ahmed M. Abu-Dief, A.A. Moniur, J. Mol. Struct., **1130**, 522−542(2017).

[31] Hany M. Abd El-Lateef, Ahmed M. Abu-Dief, Bahaa El-Dien M. El-Gendy, J.Electroanal. Chem., **758**, 135−147(2015).

[32] Hany M. Abd El-Lateef, Ahmed M. Abu-Dief, L.H. Abdel-Rahman, Eva Carolina Sañudo, NúriaAliaga-Alcalde, J. Electroanal. Chem., **743**, 120−133(2015).

[33] L. H. Abdel-Rahman, R. M. El-Khatib, L. A. E. Nassr, A. M. Abu-Dief, F. El-Din Lashin, SpectrochimicaActa Part A: Molecular Biomolecular Spectroscopy., **111**, 266–276(2013) [34] P. Kavitha, M. Rama Chary, B. V. V. A. Singavarapu, and K. Laxma Reddy, Journal of Saudi Chemical Society, 2013.

[35] Laila H. Abdel Rahman, Ahmed M. Abu‐Dief, Rafat M. El-Khatib, ShimaaMahdy Abdel-Fatah, A.M. Adam, E.M.M. Ibrahim, ApplOrganometal Chem. 2017;e4174.

[36] K. Sasikala and S. Arunachalam, Chemical Science Transactions, vol. 2, supplement., **1**, S157–S166(2013).

[37] M. Sneed and R. Brasted, Comprehensive Inorganic Chemistry, vol. 4, D. Van Nostard Company, 1965.

[38] L.H. Abdel-Rahman, A.M. Abu-Dief, M.S.S. Adam, S.K. Hamdan, Catal. Lett., **146**, 1373−1396(2016).

[39] Bjerrum, J. Metal-ammine formation in aqueous solution. Copenhagen: Haase, 1941.

[40] Laila H. Abdel-Rahman, Ahmed M. Abu-Dief, H. Mostafa, Samar KamelHamdan, Appl. Organometal. Chem., **31**, e3555(2017).

[41] Y. Prashanthi and S. Raj, Journal of Scientific Research., **2(1)**, 114–126(2010).

[42] M. Hanif and Z. H. Chohan, SpectrochimicaActa A: Molecular and Biomolecular Spectroscopy., **104**, 468–476(2013).

[43] A. W. Coats, J. P. Redfern, Nature., **68**, 201(1964).

[44] Y. J. Thakor, S. G. Patel, and K. N. Patel, Journal of Chemical and Pharmaceutical Research., **2(5)**, 518–525(2010).

[45] A. Prakash, B. K. Singh, N. Bhojak, D. Adhikari,

SpectrochimicaActa Part A ., **76**, 356(2010).

[46] (a) H. Temel, Ü. Çakir, B. Otludil, and H. I. Uğraş, Synthesis and Reactivity in Inorganic and Metal-Organic Chemistry, vol. 31, no. 8, pp. 1323–1337, 2001. (b) G.G. Mohamed and Z.H.A. E1-Wahab,SpectrochimicaActa Part A., **61**, 1059(2005).

[47] B. Manjula and S. Arul Antony, Research Journal of Chemical Sciences., **3(12)**, 22–28(2013).

[48] S. Satyanarayana, C. J. Dabrowiak, and J. B. Chairs, Biochemistry., **32(10)**, 2573–2583(1993).

[49] B. Anupama and C. GyanaKumari, International Journal of Research in Chemistry and Environment., **3(2)**, 172–180(2013).

[50] E. Akila, M. Usharani, P. Maheswaran, and R. Rajavel, International Journal of Recent Scientific Research., **4(10)**, 1497–1503(2013).